Multiwavelength variability and correlation studies of Mrk421 during historically low X-ray and γ-ray activity in 2015–2016

B. Banerjee[1], T. Terzić[2], D. Paneque[3], P. Majumdar[4] on behalf of MAGIC, *Fermi*-LAT and FACT collaborations and MWL partners.

[1]Gran Sasso Science Instiute, Viale Francesco Crispi, 7, L'Aquila (AQ), I-67100; [2]University of Rijeka, Department of Physics, 51000 Rijeka, Croatia; [3]Max-Planck-Institut für Physik, D-80805 München, Germany; [4]Saha Institute of Nuclear Physics, HBNI, 1/AF Bidhannagar, Kolkata 700064, India.

Markarian 421 (Mrk421) during 2015-2016

- Mrk 421 (redshift z=0.031) is a well studied BL Lac type object.
- Most of the studies of Mrk421 are biased towards the high flux states such as Aleksić et al. (2015) and there are only a few during non-flaring episodes (e.g., Horan et al., 2009; Abdo et al., 2011).
- During the 2015-2016 campaign, MAGIC observed the lowest flux state in the $0.2 - 1$ TeV energy range with flux value of $(3.56 \pm 0.91) \times 10^{-11}$ ph cm^{-2} s^{-1}, on MJD 57422. In X-rays, on MJD 57364, we observed the lowest ever flux in the $2 - 10$ keV band ($2.41 \pm 0.15 \times 10^{-11}$ erg cm^{-2} s^{-1}).

MWL data

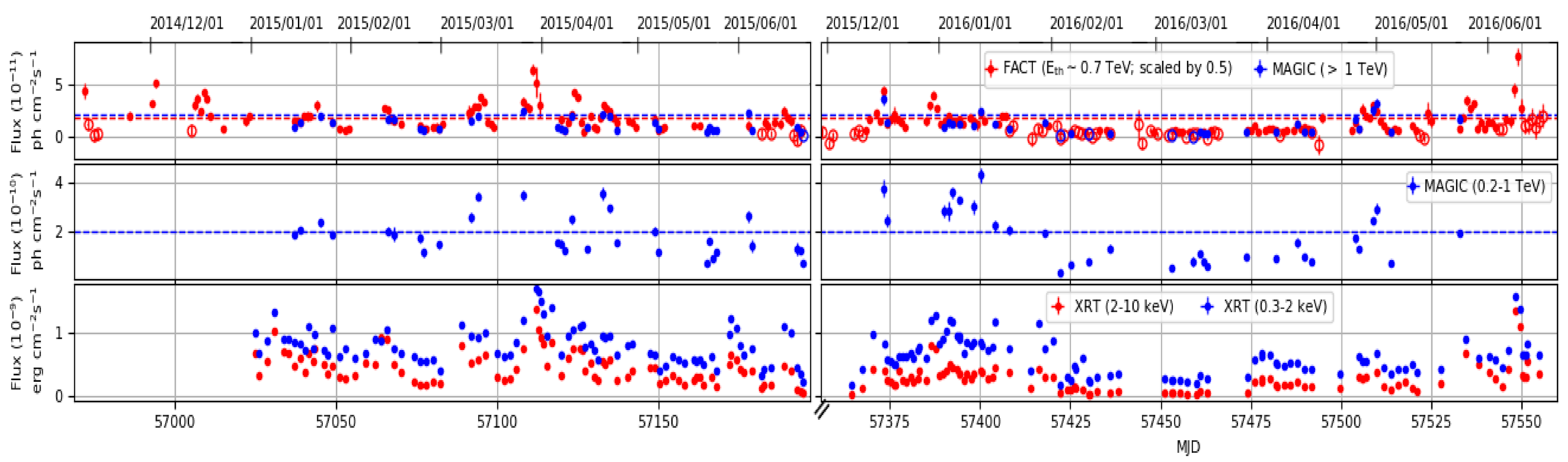

Figure 1. The VHE γ-ray (MAGIC & FACT) and X-ray lightcurves (*Swift*-XRT) during 2015–2016 campaign. Adapted from Acciari et al. (2021), Fig. 2.

- The MWL data for this work were taken from 2014 November to 2016 June.
- The dense data coverage in X-ray and very high energy (VHE; E>100 GeV) γ-rays is shown in Fig. 1.
- The details of the data analysis and data coverage are reported in Acciari et al. (2021).
- For the correlation studies on energy bands with lower variability (radio, optical, HE γ—rays), we also added data from the 2007-2014 period Acciari et al. (2021).
- The longer data set of 2007-2016 has also been used for the studies related to the flux distribution.

Hard X-ray excess

■ Synchrotron bump of Mrk421 (consisting of optical, UV, and X-ray) fitted with a log-parabola.

■ Flux measurements by *Swift*-BAT are significantly higher than the extrapolated XRT spectra during MJD 57422–57429 (Fig. 2).

■ Possible origin:

– Occasionally appearing narrow spectral component (as seen in Mrk 501; Acciari et al., 2020).

– The onset of the SSC component (Kataoka & Stawarz, 2016).

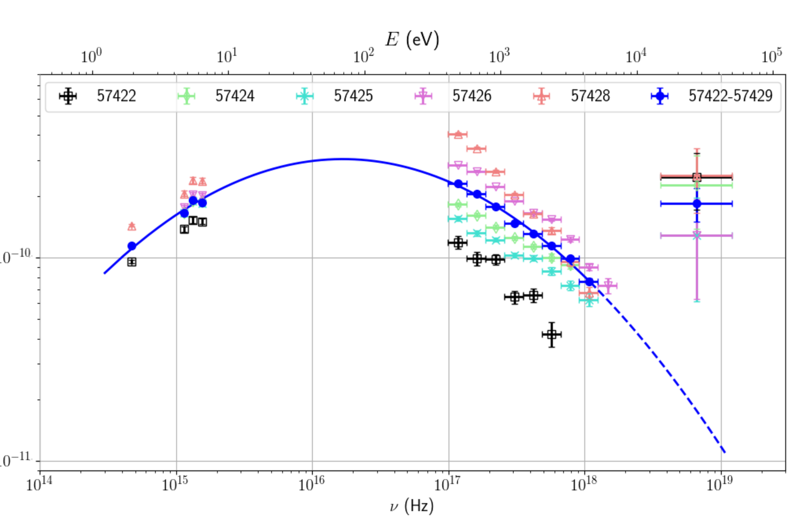

Figure 2. Log-parabola fit to the synchrotron spectrum of Mrk421 during MJD 57422-57429. From Acciari et al. (2021), Fig. 9.

Unusual radio flare at 37 GHz by Metsähovi

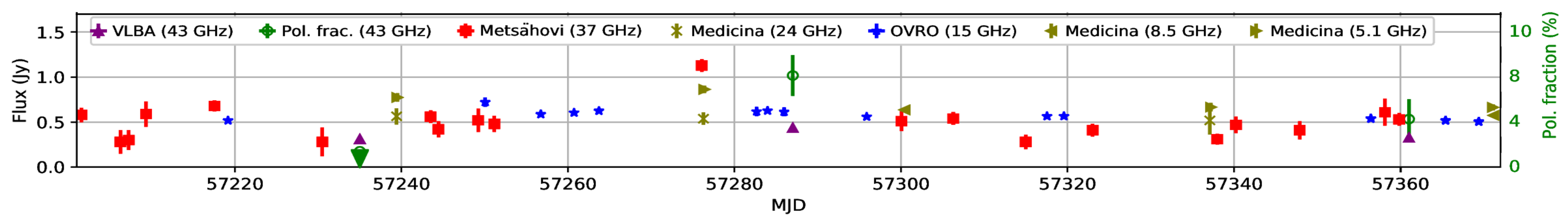

Figure 3. Radio flare detected by Metsähovi (37 GHz). From Acciari et al. (2021), Fig. 3.

■ Radio flare @37 GHz (Metsähovi) on 2015 September 11; flux doubling timescale $<$ 21 days.

■ No change in the flux observed at 24 GHz; enhanced activity at 5 GHz, both observed with Medicina.

■ Increase in the polarization fraction with VLBA on September 22.

■ This increase in flux and polarization may be caused by a momentary disruption of the ordering of the magnetic field followed by a particle-acceleration via a kink instability.

Variability and correlation

–Variability quantified with fractional variability and hardness ratio (HR=hard band flux/ soft band flux).

■ Flattening of HR vs. flux in the VHE γ—rays; pronounced in the soft VHE band. See Fig. 4.

■ Similar phenomena in the high (and low) X-ray fluxes reported in Baloković et al. (2016).

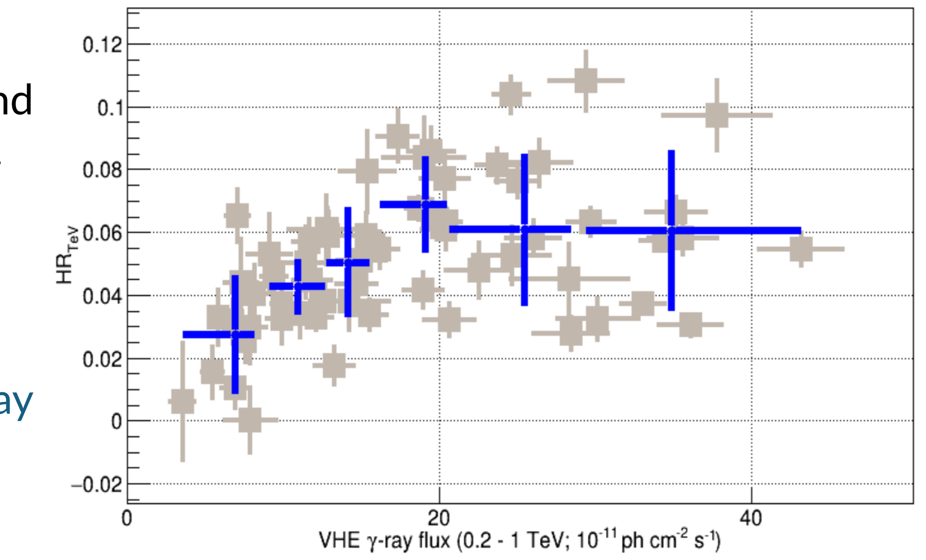

Figure 4. Flattening of HR in the VHE γ-ray band ($HR_{TeV} = \frac{Flux_{>0.1\,TeV}}{Flux_{0.2-1\,TeV}}$). From Acciari et al. (2021), Fig. 7.

– Correlation between MWL LCs quantified using Pearson and Discrete Correlation Coefficient.

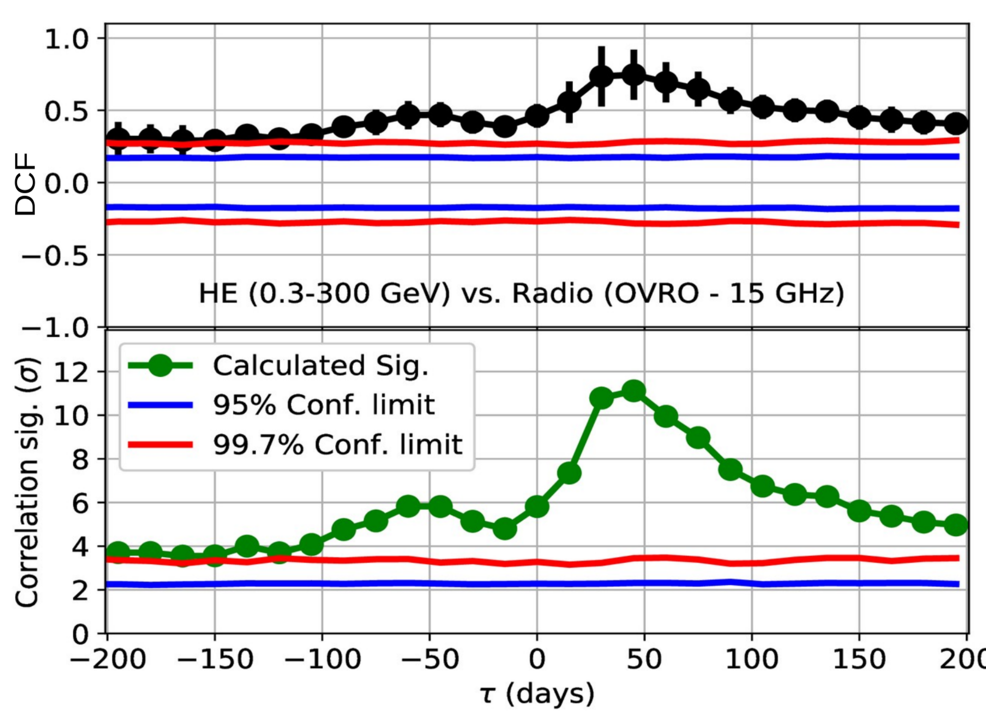

Figure 5. Correlation between the radio (OVRO; 15 GHz) and the HE γ—rays, which peaks at around 45 days. Figure from Acciari et al. (2021), Fig. 12.

The correlation results involving radio, optical and GeV bands derived from data from 2007–2014.

– There are three distinct natures of correlation emerging from this study: Correlation between

■ X-ray and VHE γ-ray at time-lag τ=0, with a significance above 5σ;

■ Optical and HE γ-rays at τ=0, with a significance $\sim$11σ;

■ Radio and HE (and optical) LCs at $\sim$45-d, with a significance $\sim$11σ; see Fig. 5.

Flux distribution using "Flux-profile" & "Unbinned likelihood" methods

– Flux distribution study provides hints about the underlying processes in the jets.

■ Crucial drawbacks of flux-histograms using χ^2 minimization:

a) Highly dependent on the choice of the binning, and b) Flux uncertainty not considered.

– Two newly devised methods that consider flux uncertainties, and no binning required:

■ Flux-profile: Calculate Gaussians for each observation with flux as the mean and flux-error as the std. deviation. Add them to obtain the flux profile. Fit the profile with the Gaussian and LogNormal functions (Acciari et al., 2021). The goodness of fit is obtained with the squared sum of the residuals.

■ Unbinned log-likelihood: Construct two unbinned log-likelihood functions: Gaussian PDF and LogNormal PDF (Acciari et al., 2021) with the data and calculate the log-likelihood for fitting.

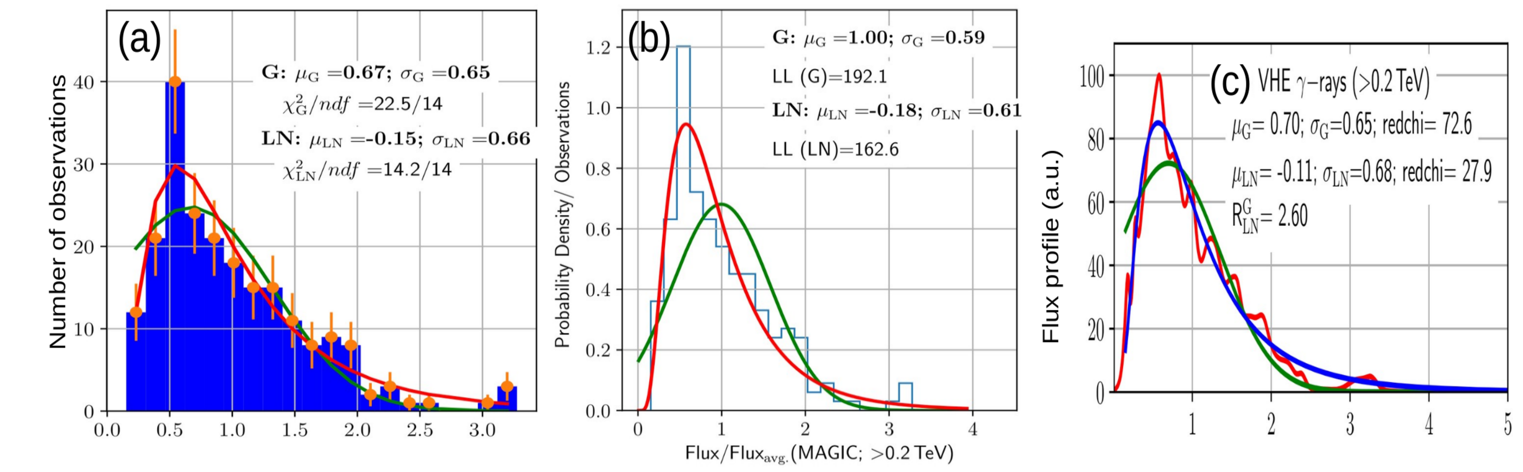

Figure 6. Flux distribution of Mrk421 in the VHE γ-rays using: (a) χ^2 minimization, (b) Log-likelihood, and (c) Flux profile methods. From Acciari et al. (2021), Fig. 13, E2, and G2.

- Most probable states are close to the average flux for the radio, optical and soft X-rays (bands below the synchrotron and inverse-Compton bumps). Differs for hard X-rays and VHE γ-rays (bands above the two SED bumps).
- The flux distributions in radio and soft X-rays better described with Gaussian, while the rest are better described with LogNormal.
- A LogNormal distribution suggests that multiplicative process are responsible for variability (e.g., fluctuations in the accretion disk; McHardy, 2010).

References

Abdo A. A., et al., 2011, ApJ, 736, 131
Acciari et al. V. A., 2020, A&A, 637, A86
Acciari et al. V. A., 2021, MNRAS, 504, 1427
Aleksić et al. 2015, A&A, 578, A22
Baloković et al. M., 2016, ApJ, 819, 156
Horan et al. D., 2009, ApJ, 695, 596
Kataoka J., Stawarz Ł., 2016, ApJ, 827, 55
Max-Moerbeck et al. W., 2014, MNRAS, 445, 428
McHardy I., 2010, X-Ray Variability of AGN and Relationship to Galactic Black Hole Binary Systems. p. 203, doi:10.1007/978-3-540-76937-8_8
Petropoulou M., Coenders S., Dimitrakoudis S., 2016, Astroparticle Physics, 80, 115
van den Berg et al. J. P., 2019, ApJ, 874, 47

Acknowledgement

The MAGIC collaboration acknowledges the support from the agencies and organizations listed here:`https://magic.mpp.mpg.de/acknowledgments_ICRC2021/`. The FACT collaboration acknowledges the support from the agencies and organizations listed here: `https://fact-project.org/collaboration/icrc2021_acknowledgements.html`. BB acknowledges financial support from MIUR (PRIN 2017 grant 20179ZF5KS).